Stability of square oscillations in a delayed-feedback system

Michel Nizette
Theoretical Nonlinear Optics, Université Libre de Bruxelles, CodePostale 231, Boulevard du Triomphe, B-1050 Brussels, Belgium
(Received 31 March 2004; revised manuscript received 17 August 2004; published 10 November 2004)

A semianalytical theory of the stability of odd-harmonic square oscillation modes of a nonlinear delayed-feedback system operating in the period-2 regime is proposed. Stability is found to be ruled by how the system approaches or leaves plateaus. An organization of the stability domains in interrupted bands of values of the delay is revealed.

DOI: 10.1103/PhysRevE.70.056204 PACS number(s): 05.45.−a, 42.65.Sf, 02.30.Ks, 42.65.Pc

I. INTRODUCTION

Dynamical systems subject to delayed feedback have received a growing interest over the past decades. They arise in various research fields such as population dynamics [1], physiological diseases [2], or neuron system modeling [3,4]. In optics, delayed feedback occurs as a result of the finite speed of light, when an optical signal is allowed to propagate over a closed path. Famous, well-studied examples of such systems include the external-cavity semiconductor laser [5] and the Ikeda optical ring cavity [6,7]. The latter is known, in particular, for its ability to exhibit a manifold of multistable temporal oscillation patterns [8]. Studies of electro-optical bistable devices have explored the potential applicability of this phenomenon for large-capacity optical signal storage [9–12]. Successful realizations were reported, but also revealed that the stability of the information-carrying patterns is a very complex issue [10]. More recently, electro-optical bistable devices have been proposed as receiver-transmitter pairs for secure communication schemes based on chaos synchronization [13–15]. Although primarily focused on chaotic operation, these studies contribute to boost the scientific community's interest in a fundamental knowledge of the dynamics of these systems, including the nonchaotic regimes [16].

The present paper aims at improving our understanding of the stability of the periodic patterns generated by electro-optical bistable devices and exploited in information storage experiments. In the past, fair agreement between experimental results and numerical simulations has been obtained, allowing the checking of a good many theoretical predictions [6–12,17–20]. However, a fundamental knowledge of the mechanisms ruling stability is lacking. Even in the absence of external influences, it is still partially unclear when and why a particular pattern acquires or loses stability. This paper contributes to overcome this limitation by proposing a semi-analytical theory of the stability, in the *period-2* (P2) domain. This term refers to an operation regime characterized by square oscillations with a period T slightly larger than twice the delay. [A typical P2 output is displayed in Fig. 1(a).] The fundamental mode shown there often coexists with its odd harmonics [see the third harmonic in Fig. 1(b)]. These modes can undergo successive period-doubling bifurcations, making them precursors to the larger-period patterns usable for information storage.

The simplest models of electro-optical bistable devices consist of a delay-differential equation of the (dimensionless) form

$$\dot{x}(t) + x(t) = f(x(t-r)), \tag{1}$$

where a dot means differentiation with respect to time t, r is the delay, x represents the output signal, and the function f accounts for the nonlinear response of the device and may depend on a number of controllable parameters [13–15,20]. Similar equations (or systems thereof) also arise as models for electronic circuits [21] or neuron systems [3,4]. A well documented model is Ikeda's equation, for which $f(z) \equiv \pi\mu[1+2B\cos(z-x_0)]$ [19]. The analysis presented here is carried out for the generic model (1). However, all quantitative results displayed in the form of diagrams pertain to Ikeda's equation with $B=0.5$ and $x_0=-\pi/2$. These values are chosen so as to allow a direct comparison with Ref. [19]. The equation then reduces to

$$\dot{x}(t) + x(t) = \pi\mu[1 - \sin x(t-r)], \tag{2}$$

where the delay r and the pumping rate μ are the only remaining free parameters.

II. TRANSIENT DYNAMICS

The study of delay-differential equations is challenging. However, analogies between delayed and spatially extended systems have been unraveled [22] and open the way to new methods of analysis [23]. A bidimensional representation of temporal data has been useful for the discovery of these analogies [24]. In Fig. 2, long-lived transient oscillations of

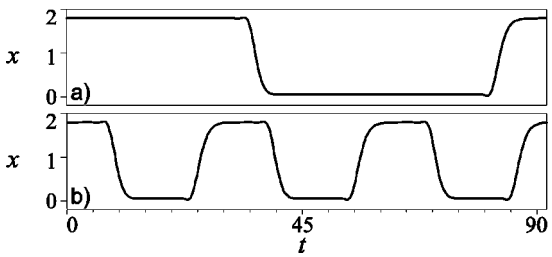

FIG. 1. Periodic solutions of Ikeda's equation (2) in the P2 regime for $\mu=0.6$ and $r=45$. The horizontal axis spans one fundamental period T, which is slightly larger than twice the delay.

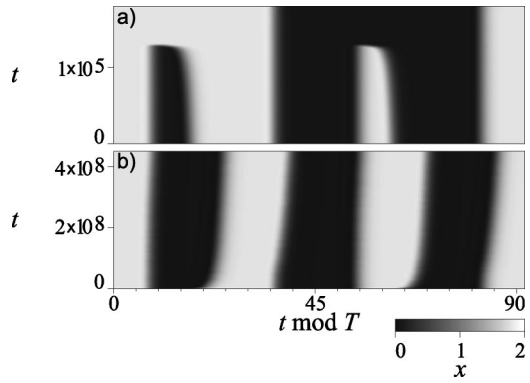

FIG. 2. Transient solutions of Ikeda's equation (2) in a bidimensional temporal data representation (see text) for $\mu=0.6$ and $r=45$. Values of x are represented on a gray scale.

Eq. (2) are analyzed using such a representation. Two numerical solutions of Eq. (2) with $\mu=0.6$ corresponding to distinct initial conditions are represented in the plane t vs (t mod T), the values of x being measured on a gray scale. [The *fundamental period* T has been first determined from the fundamental P2 solution of Eq. (2) shown in Fig. 1(a).] Figure 2 separates visually the fast square oscillations over a time interval T, measured along the horizontal axis, from the much slower transient dynamics observable along the vertical axis. The dynamics is structured as an alternance of plateaus connected by slowly drifting domain walls. Figure 2(a) features the attraction, collision, and annihilation of two pairs of opposite walls. This leads to the establishment of a periodic final state with only two walls per period, identifiable as the fundamental mode shown in Fig. 1(a). In Fig. 2(b), no such annihilation takes place as adjacent walls actually repel each other. There the final state is the third harmonic with equispaced transitions shown in Fig. 1(b). Figure 2 thus illustrates a case of bistability between the fundamental mode and its third harmonic, by showing that both modes are reachable from appropriate initial conditions.

Figure 3 offers an alternative representation of the same dynamics. There, the distribution of the *transition times* t_k (k integer) is plotted in the plane t vs $\left[t \bmod \left(\frac{1}{2}T\right)\right]$. The t_k are defined precisely as the Poincaré times satisfying the condition $x(t_k)=x\left(t_k-\frac{1}{2}T\right)$. Note how their distribution follows the motion of the domain walls in Fig. 2. This suggests that the

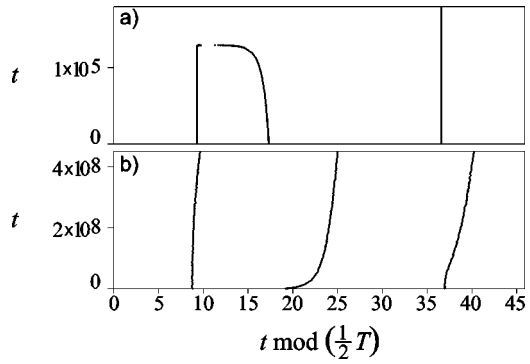

FIG. 3. Distributions of the transition times extracted from the data of Fig. 2.

clue to the stability of the oscillation patterns lies in the analysis of how the distribution of the transition times over a half period determines its own drift on a large time scale. However, direct numerical integration of Eq. (1) can be impractical for this purpose, given how large the required integration time typically is, even with modern equipment. Indeed, in the P2 regime, one must keep in mind that transient times tend to grow exponentially as functions of the delay [25]. This is exemplified by the ordinate scales of Figs. 2 and 3 , which give measures of the stiffness of the problem. Care must be taken to deal with this difficulty properly, as failing to do so could lead to incorrect interpretations of numerical data. Numerical continuation methods could also be tricky to put in practice, as exponentially large transient times implies nearly marginal stability. What is required, then, is the analytical derivation from Eq. (1) of a recurrence relation for the Poincaré times t_k.

III. ANALYSIS

Consider a solution x of Eq. (1). In the P2 regime, x switches between two plateau values x_0 and x_1 ($x_0<x_1$) given approximately by

$$x_0 = f(x_1), x_1 = f(x_0). \tag{3}$$

Let n denote the number of such transitions per half period. Feedback forces the solution x to repeat itself with a plateau inversion every half period, implying that n is an odd number. [The fundamental mode of Fig. 1(a) and its third harmonic in Fig. 1(b) correspond to $n=1$ and 3, respectively.] Our analysis rests on the two following assumptions.

Hypothesis 1: successive transitions are well separated in time. This means that the intervals t_k-t_{k-1} between transitions are significantly larger than the duration of a transition, denoted 2Δ. This implies, in particular, that the delay r is large compared to 2Δ.

Hypothesis 2: the solution x is almost periodic with period T. Specifically, $t_k-t_{k-n}\simeq\frac{1}{2}T$ for all k.

We want to show that the behavior of the solution x of Eq. (1) during transitions plays an important role in the long-term dynamics. Transitions are described approximately by a pair of transition layer equations [26] as follows. Let $u_0(t)$ and $u_1(t)$solve the system

$$\dot{u}_0(t) + u_0(t) = f(u_1(t+a)), \tag{4a}$$

$$\dot{u}_1(t) + u_1(t) = f(u_0(t+a)), \tag{4b}$$

with conditions

$$u_0(-\infty) = u_1(+\infty) = x_0, \quad u_1(-\infty) = u_0(+\infty) = x_1,$$

$$u_0(0) = u_1(0). \tag{5}$$

The symbol a in Eqs. (4) is an unspecified constant. A solution $\{u_0, u_1\}$ does not exist for arbitrary values of a, so that a must be determined, as part of the problem, so as to render Eqs. (4) and (5) solvable. Then, u_0 and u_1 describe, respectively, the upwards and downwards transitions. More precisely, the solution x of Eq. (1) is well approximated by

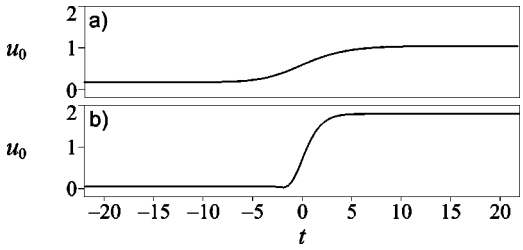

FIG. 4. Upwards transition layer u_0 for Ikeda's equation (2) with (a) $\mu=0.4$, (b) $\mu=0.6$.

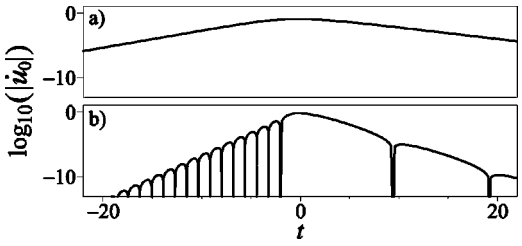

FIG. 5. Logarithm of the slope $|\dot{u}_0|$ of the upwards transition layer u_0 for Ikeda's equation (2) with (a) $\mu=0.4$, (b) $\mu=0.6$.

$x(t) \simeq u_k(t-t_k)$ for $|t-t_k| \lesssim \Delta$, where $u_k \equiv u_{k \bmod 2}$, for all k. The upwards transition layer u_0 for Ikeda's equation (2) is shown in Fig. 4 for two distinct values of μ. [It can be checked that Fig. 4(b) describes well the upwards transitions in Fig. 1, where the same value of μ is used.] Furthermore, the relation

$$a = \frac{1}{2}T - r \tag{6}$$

is known to hold for large r, so that a can be thought of as the lag of the half period with respect to the delay.

In general, no explicit analytical expressions exist for the unknowns $u_0(t)$, $u_1(t)$, and a of the problem (4) and (5), which then have to be determined numerically. Useful information about the *tails* of the transition layers (i.e., the asymptotic behaviors of the transition layers u_0 and u_1 beyond or ahead of the transition) can, nevertheless, be obtained from a linearized form of Eqs. (4), as follows. Substituting $u_0(t)=u_0(\pm\infty)+\varepsilon_0 \exp(\sigma t)$ and $u_1(t)=u_1(\pm\infty)+\varepsilon_1 \exp(\sigma t)$ in Eqs. (4) and keeping only linear contributions in the constants ε_0, ε_1 leads to

$$(\sigma+1)\varepsilon_0 = f'(u_1(\pm\infty))\varepsilon_1 \exp(\sigma a), \tag{7a}$$

$$(\sigma+1)\varepsilon_1 = f'(u_0(\pm\infty))\varepsilon_0 \exp(\sigma a), \tag{7b}$$

where the prime denotes differentiation. The ± sign determines whether the equations above are relevant beyond or ahead of a transition. Requiring that Eqs. (7) admit nontrivial solutions $\{\varepsilon_0, \varepsilon_1\}$ yields an equation for the eigenvalues σ (which happens to be independent of the ± sign)

$$(\sigma+1)^2 = \lambda \exp(2\sigma a), \tag{8}$$

where $\lambda \equiv f'(x_0)f'(x_1)$. Let σ_- and σ_+ be respectively the eigenvalues with the greatest negative and smallest positive real parts. They represent the exponential decay rates of the *future* and *past* tails of the transition layers, respectively. Specifically, one can write (compactly)

$$\left.\begin{aligned} u_0(t) &= u_0(\pm\infty) + \mathcal{R}_{\mp}[A_0^{\pm} \exp(\sigma_{\mp} t)] \\ u_1(t) &= u_1(\pm\infty) + \mathcal{R}_{\mp}[A_1^{\pm} \exp(\sigma_{\mp} t)] \end{aligned}\right\} \quad \text{for} \pm t \gtrsim \Delta, \tag{9}$$

where $A_0^{\pm}$, $A_1^{\pm}$ are four constant amplitudes, and where the shorthand notations $\mathcal{R}_{\mp}[z]$ represent z if $\sigma_{\mp}$ is real and $z+z^*$ otherwise (star denoting complex conjugation). The amplitudes $A_0^{\pm}$, $A_1^{\pm}$ cannot be completely determined from the linear analysis.

For a large enough delay r, the conditions of P2 oscillation for Eq. (1) closely match those for the discrete map obtained by setting the left-hand side of Eq. (1) to zero [27]. In particular, one has approximately $\lambda=1$ at the P2 oscillation threshold and $\lambda=-1$ at a period-4 bifurcation. Now, an analysis of Eq. (8) reveals that both eigenvalues $\sigma_{\pm}$ are real if $\lambda>0$ and both have an imaginary part if $\lambda<0$. From this, we infer that the tails start out monotonous at the P2 threshold and become oscillatory at some point (i.e., at $\lambda=0$) along the route to period 4. The presence or absence of tail oscillations is illustrated in Fig. 5, where the slope $|\dot{u}_0|$ of the upwards transition layer is shown for Ikeda's equation (2) for two different values of μ. The logarithmic scale used is necessary to reveal the absence [Fig. 5(a)] or presence [Fig. 5(b)] of oscillations efficiently. The feature can barely be discerned from Fig. 4 where μ_0 is plotted on a linear scale for the same values of μ. Its importance nevertheless becomes clear in the following.

Using hypothesis 2 and the relation (6), $t_k - t_{k-n}$ can be written as

$$t_k - t_{k-n} \equiv r + a + \delta_k, \tag{10}$$

where the δ_k represent small unknown deviations of the transition times from one half period to the next. If the δ_k can be determined, then they give a recurrence relation for the transition times t_k, which solves our problem. The transition layers $u_k(t-t_k)$ provide a first approximation to the solution x of Eq. (1) during transitions. This motivates Ansätze of the form $x(t)=u_k(t-t_k)+\xi_k(t-t_k)$, where the ξ_k represent small corrections to the transition layers u_k. It is possible to derive a system of equations for the ξ_k and to formulate the boundary conditions they have to satisfy. However, the existence of solutions to the resulting problem is not ensured; one thus has to impose it explicitly as conditions over its parameters. We have found that these solvability conditions determine the deviations δ_k. The resulting equations for the δ_k can be expressed in terms of the solution of an auxiliary nonautonomous linear problem, as follows. Consider the system

$$-\dot{v}_0(t) + v_0(t) = v_1(t-a)f'(u_0(t)), \tag{11a}$$

$$-\dot{v}_1(t) + v_1(t) = v_0(t-a)f'(u_1(t)). \tag{11b}$$

We can show that, generically, a bounded solution $\{v_0, v_1\}$ of these equations behaves asymptotically as

$$\left.\begin{aligned} v_0(t) &= \mathcal{R}_\pm[B_0^\pm \exp(-\sigma_\pm t)] \\ v_1(t) &= \mathcal{R}_\pm[B_1^\pm \exp(-\sigma_\pm t)] \end{aligned}\right\} \text{ for } \pm t \gtrsim \Delta, \qquad (12)$$

where $B_0^\pm$, $B_1^\pm$ are some constants. Assume that the solution $\{v_0, v_1\}$ is normalized so that

$$\int_{-\infty}^{+\infty} dt[v_1(t-a)f'(u_0(t))\dot{u}_0(t) + v_0(t-a)f'(u_1(t))\dot{u}_1(t)] = 1. \qquad (13)$$

This normalization is chosen so as to make some expressions below as simple as possible. Equations (11)–(13) determine $B_0^\pm$ and $B_1^\pm$ completely. Then, a calculation reveals the δ_k to be given by

$$\delta_k = F_-(t_k - t_{k-1}) + F_+(t_k - t_{k+1}), \qquad (14)$$

where

$$F_\pm(t) \equiv \mathcal{R}_\pm[C^\pm \exp(\sigma_\pm t)], \qquad (15)$$

$$C^\pm \equiv \pm (B_0^\pm A_1^\mp + B_1^\pm A_0^\mp)[1 - (1 + \sigma_\pm)a]. \qquad (16)$$

Equations (10) and (14) together yield the sought recurrence relation for the transition times t_k. It is then convenient to express the t_k in terms of new variables more directly related to the bidimensional data representations of Fig. 3. Let $s_k^l \equiv t_{nl+k} - (r+a)l$, where $k = 0, \ldots, n-1$ and l is any integer. The variable s_k^l then represents the *displacement* of the kth transition after l half periods. In those parts of Fig. 3 where the number n of transitions per half period is conserved, s_l^k can be read directly as the kth abscissa corresponding to ordinate $t = (r+a)l$. Because $\delta_{nl+k} = s_k^l - s_k^{l-1}$ is a small quantity, the variables s_k^l differ little from one value of l to the next. Therefore it makes sense to replace the discrete index l with a continuous time variable: $l = t/(r+a)$, and to approximate discrete differences as time derivatives: $\delta_{nl+k} = s_k^l - s_k^{l-1} = (r+a)\dot{s}_k(t)$. In terms of the new variables, the system formed by Eqs. (10) and (14) becomes

$$(r+a)\dot{s}_k = F_-(s_k - s_{k-1}) + F_+(s_k - s_{k+1}),$$

$$k = 0, \ldots, n-1, \qquad (17)$$

where we have defined $s_{-1} \equiv s_{n-1} - (r+a)$ and $s_n \equiv s_0 + (r+a)$.

IV. RESULTS

Equations (17) form a finite set of ordinary differential equations. They relate the slow drift of the transitions to the time intervals separating them. Stable P2 solutions of Eq. (1) correspond to stable equilibria of Eqs. (17). The terms $F_\pm$ in the right-hand side can be interpreted as accounting for effective interactions between adjacent domain walls, that lead to the formation of dissipative structures as depicted by Fig. 2. The sign and magnitude of the interactions depend on the wall separation. The description of the evolution of the oscillation pattern offered by Eqs. (17) bears a high similarity with the dynamics of a spatial distribution of pointlike particles. From Eq. (15), we see that the interactions $F_\pm$ decrease exponentially (at rates $|\sigma_\pm|$) with wall separation. The decrease is either monotonous or oscillatory, in direct relation to the shapes of the transition layer tails. It is possible to prove from Eqs. (4) and (11) that, as long as the tails remain monotonous, the interaction terms $F_\pm$ are always attractive. In that case, a stability analysis of Eqs. (17) reveals that any solution with $n > 1$ is unstable. The walls thus tend to collapse and annihilate by pairs until there remains only one wall per half period. This implies that the only possible stable pattern is the fundamental mode if the front tails are monotonous. Such a dynamics is comparable to that of attractor particles constrained to move on a circle: if there are more than one particle, then they will collapse by pairs until there is only one particle left. On the other hand, if the transition layer tails oscillate, then so do the interaction terms $F_\pm$ as a function of wall separation. In that case, multiple stable equilibria, corresponding to different values of n, are possible. In conclusion, *in the absence of external perturbations, the stability of the higher harmonics* $(n > 1)$ *is determined by the asymptotic behavior of the system beyond or ahead of transitions*.

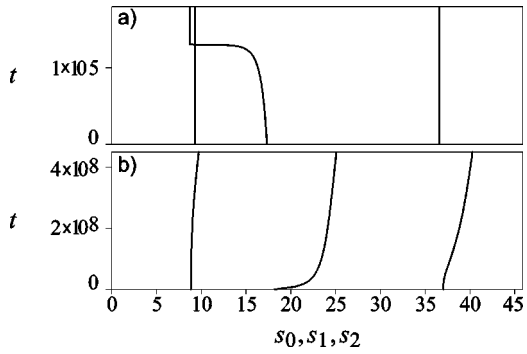

FIG. 6. Solutions $\{s_0(t), s_1(t), s_2(t)\}$ of Eqs. (17) for $n=3$ and two different initial conditions. Parameter values in Eqs. (17) have been computed so as to correspond to Ikeda's equation (2) for $\mu = 0.6$ and $r = 45$. Compare with Fig. 3.

In order to make quantitative predictions, the constants a, $\sigma_\pm$, and $C^\pm$ appearing in Eqs. (14)–(16) have to be evaluated. This requires the knowledge of solutions to the problems (4) and (11). Their numerical computation is easy enough (if tackled properly) and free from the difficulty of dealing with exponentially long transients. As a test of the validity of the wall drift equations (17), we have undertaken to reproduce the transition time distributions plotted in Fig. 3. The parameters a, $\sigma_\pm$, and $C^\pm$ have been evaluated for Ikeda's equation (2) for $\mu = 0.6$, and Eqs. (17) have been integrated for $n=3$, $r=45$, and suitable initial conditions. Then, diagrams have been constructed with time t appearing as the ordinate and $s_0(t)$, $s_1(t)$, and $s_2(t)$ plotted along the horizontal axis. The resulting curves, shown in Fig. 6, are nearly indistinguishable from the corresponding plots in Fig. 3, except in the vicinity of the front pair annihilation in Fig. 3(a) and beyond, where Eqs. (17) lose their validity due to the violation of Hypothesis 1. The nearly P2 dynamics of the original system (2) is thus very accurately described by the simplified equations (17), whose integration is an incomparably less stiff problem.

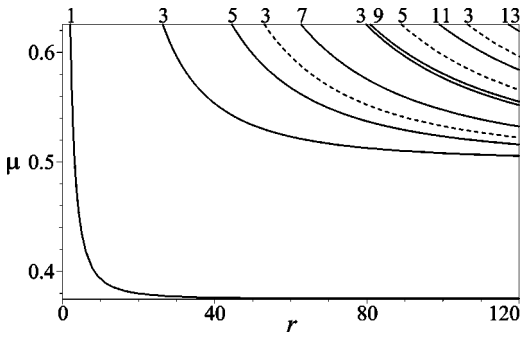

FIG. 7. Stability boundaries of the regular oscillation modes of Ikeda's equation (2), in the P2 regime. Numbers indicate the order n of the harmonic undergoing a stability change. The stability domains are located to the right (respectively left) of solid (respectively dashed) curves.

We now use Eqs. (17) to analyze the stability of the P2 oscillation modes of Eq. (2) with equispaced transitions: $s_k - s_{k-1} = (r+a)/n$ for $k = 0, \ldots, n-1$. For Ikeda's equation (2), the P2 oscillation threshold μ_2 and the period-4 biifurcation μ_4 are given, for large r, by $\mu_2 = 0.374$ and $\mu_4 = 0.626$. Furthermore, the change from monotonous tails to oscillatory tails occurs at $\overline{\mu_2} = 0.5$. Figure 7 shows the stability boundaries of the first few harmonic modes in the μ vs r plane for $\mu_2 < \mu < \mu_4$. The stability of the higher harmonics ($n > 1$) has been determined from Eqs. (17) for a sample of values of μ between $\overline{\mu_2}$ and μ_4. The results were interpolated to obtain the smooth curves shown in the diagram. The stability boundary of the fundamental mode $n = 1$ was determined from Eq. (2) linearized about the steady state. Figure 7 can be directly compared to Fig. 4 in Ref. [19]. Although both figures agree qualitatively in their overlapping parts, the latter tends to overestimate the stability domains of the higher harmonics. Discrepancies of this nature are not unexpected in view of the very long transient times in the system. Note, in particular, that Ref. [19] predicts asymptotes at $\mu = \mu_2$ for the stability boundaries of all modes, whereas Fig. 7 predicts an asymptote at $\mu = \mu_2$ for $n = 1$ and asymptotes at $\mu = \overline{\mu_2}$ for the higher harmonics.

Note also from Fig. 7 that the stability domain for fixed μ or a specific harmonic n is structured in disconnected *bands* of values of r. Each band is bounded to the left by a numbered solid curve and to the right by an identically numbered dashed curve. The band structure in Fig. 7 can be best observed for the third harmonic, whose first two stability bands are displayed. From Eqs. (17), we compute that the size and separation of the stability bands for the nth harmonic is given approximately by $n\pi/\mathrm{Im}(\sigma_-)$, which corresponds to the duration of n half cycles in the oscillations of the transition layers' future tails. [Compare the band sizes at $\mu = 0.6$ in Fig. 7 with the size of the humps in the right part of Fig. 5(b), which represent successive half cycles in the future tail.] This latter result can be established without reference to particular values of the parameters in Eqs. (17). Consequently, it is not specific to Ikeda's equation (2), but is generic for equations of the form Eq. (1). The identification and quantitative characterization of this band structure is an important achievement as it underlines the necessity of choosing the delay properly in order to stabilize a given harmonic. Even if the system is adequately insulated from external influences, an inappropriate delay can cause an instability.

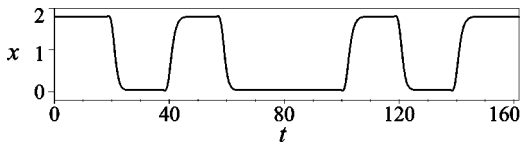

FIG. 8. A stable periodic solution of Ikeda's equation (2) for $\mu = 0.6$ and $r = 80$. In contrast to the P2 patterns shown in Fig. 1, this one has irregularly sized plateaus. The horizontal axis spans one period.

The regular patterns with equispaced transitions, illustrated in Fig. 1, are not the only possible stable solutions. Figure 8 shows an example of a stable periodic solution of Ikeda's equation (2) with irregularly sized plateaus. Again, its stability has been established using the front drift equations (17). To our knowledge, the ability of Ikeda's equation to generate irregular patterns in the P2 regime has never been predicted before.

V. CONCLUSIONS

In this paper, we have identified the factors determining the stability of the square oscillation modes of a delayed-feedback system isolated from external influences. These factors have been tracked down to the asymptotic behavior of the system beyond or ahead of transitions. The domain of stability of each mode was found to be organized in bands of values of the delay. The size of these bands has been related to the duration of the damped oscillation cycle as the system approaches a plateau. Moreover, the existence of P2 patterns with irregularly sized plateaus has been predicted. The principle of the analysis is fairly easily extensible for the taking into account of external perturbations. The strategy for its extension to the period-4 regime and beyond remains to be investigated.

ACKNOWLEDGMENTS

This work was funded by the Belgian National Fund for Scientific Research and by the IAP program of the Belgian government. The author acknowledges enlightening discussions with Professor Thomas Erneux and Professor Rajarshi Roy.

[1] R. M. May, Nature (London) **261**, 459 (1976).
[2] M. C. Mackey and L. Glass, Science **197**, 287 (1977).
[3] C. M. Marcus and R. M. Westervelt, Phys. Rev. A **39**, 347 (1989).
[4] J. Foss, A. Longtin, B. Mensour, and J. Milton, Phys. Rev. Lett. **76**, 708 (1996).
[5] R. Lang and K. Kobayashi, IEEE J. Quantum Electron. **QE–16**, 347 (1980).
[6] K. Ikeda, Opt. Commun. **30**, 257 (1979).
[7] K. Ikeda, H. Daido, and O. Akimoto, Phys. Rev. Lett. **45**, 709 (1980).
[8] M. W. Derstine, H. M. Gibbs, F. A. Hopf, and D. L. Kaplan, Phys. Rev. A **27**, 3200 (1983).
[9] K. Ikeda and K. Matsumoto, Physica D **29**, 223 (1987).
[10] T. Aida and P. Davis, IEEE J. Quantum Electron. **28**, 686 (1992).
[11] T. Aida and P. Davis, IEEE J. Quantum Electron. **30**, 2986 (1994).
[12] Y. Zhang, J.-B. Li, Z.-R. Zheng, Y. Jiang, and J.-Y. Gao, Phys. Rev. E **57**, 1611 (1998).
[13] J.-P. Goedgebuer, L. Larger, and H. Porte, Phys. Rev. Lett. **80**, 2249 (1998).
[14] L. Yaowen, G. Guangming, Z. Hong, W. Yinghai, and G. Liang, Phys. Rev. E **62**, 7898 (2000).
[15] V. S. Udaltsov, J.-P. Goedgebuer, L. Larger, and W. T. Rhodes, Phys. Rev. Lett. **86**, 1892 (2001).
[16] L. Larger, M. W. Lee, J.-P. Goedgebuer, W. Elflein, and T. Erneux, J. Opt. Soc. Am. B **18**, 1063 (2001).
[17] H. M. Gibbs, F. A. Hopf, D. L. Kaplan, and R. L. Shoemaker, Phys. Rev. Lett. **46**, 474 (1981).
[18] F. A. Hopf, D. L. Kaplan, H. M. Gibbs, and R. L. Shoemaker, Phys. Rev. A **25**, 2172 (1982).
[19] K. Ikeda, K. Kondo, and O. Akimoto, Phys. Rev. Lett. **49**, 1467 (1982).
[20] R. Vallée and C. Delisle, Phys. Rev. A **34**, 309 (1986).
[21] L. Larger, J.-P. Goedgebuer, and T. Erneux, Phys. Rev. E **69**, 036210 (2004).
[22] G. Giacomelli and A. Politi, Phys. Rev. Lett. **76**, 2686 (1996).
[23] M. Nizette, Physica D **183**, 220 (2003).
[24] F. T. Arecchi, G. Giacomelli, A. Lapucci, and R. Meucci, Phys. Rev. A **45**, 4225 (1992).
[25] C. Grotta-Ragazzo, K. Pakdaman, and C. P. Malta, Phys. Rev. E **60**, 6230 (1999).
[26] S.-N. Chow, X.-B. Lin, and J. Mallet-Paret, J. Dyn. Differ. Equ. **1**, 3 (1989).
[27] P. Nardone, P. Mandel, and R. Kapral, Phys. Rev. A **33**, 2465 (1986).